A Single-Period $TE_{02}-TE_{01}$ Mode Converter in a Highly Overmoded Circular Waveguide

Michael J. Buckley, *Member, IEEE*, David A. Stein, and Ronald J. Vernon, *Member, IEEE*

***Abstract*—A single-period 60 GHz $TE_{02}-TE_{01}$ mode converter for use in an electron cyclotron heating (ECH) system for magnetically confined plasmas is presented. The mode converter is very compact and has a broad bandwidth and a theoretical conversion efficiency of 97.6%. A method of computing the reflection from mode converters is presented and used to show that reflection from the single-period mode converter is minimal. Experimental results are consistent with theoretical calculations.**

I. Introduction

Gyrotrons are an efficient source of high-power millimeter-wavelength energy. With output powers that reach above 500 kW and frequencies that range from 28 GHz to 150 GHz and beyond, gyrotrons have been successfully used to heat magnetically confined plasmas at the electron cyclotron resonance frequency [1]–[3]. The first generation gyrotron typically has its output in an axially symmetric TE_{0n} mode in a 6.35-cm-diameter waveguide. The gyrotron's output mode is usually converted into a linearly polarized mode by means of one or more mode converters. In order for the mode converters to be of reasonable length the waveguide diameter is usually tapered form 6.35 cm to 2.779 cm.

II. $TE_{0n}-TE_{0q}$ Coupled Mode Equations

The coupled mode equations can be written in the form [4]

$$\frac{dA_n^+}{dz} = -i\beta_n(z)A_n^+ + \frac{1}{2\beta_n}\frac{d\beta_n}{dz}A_n^- + \sum_{\substack{q \\ q\neq n}} \left(T_{nq}(z)A_q^+(z) + \Gamma_{nq}(z)A_q^-(z)\right) \quad (1)$$

and

$$\frac{dA_n^-}{dz} = i\beta_n(z)A_n^- + \frac{1}{2\beta_n}\frac{d\beta_n}{dz}A_n^+ + \sum_{\substack{q \\ q\neq n}} \left(\Gamma_{nq}(z)A_q^+(z) + T_{nq}(z)A_q^-(z)\right) \quad (2)$$

where

$$T_{nq}(z) = \frac{1}{a}\frac{da}{dz}\frac{X'_{0n}X'_{0q}}{X'^2_{0n} - X'^2_{0q}}\left((\beta_q/\beta_n)^{1/2} + (\beta_n/\beta_q)^{1/2}\right) \quad (3)$$

and

$$\Gamma_{nq}(z) = \frac{1}{a}\frac{da}{dz}\frac{X'_{0n}X'_{0q}}{X'^2_{0n} - X'^2_{0q}}\left((\beta_q/\beta_n)^{1/2} - (\beta_n/\beta_q)^{1/2}\right). \quad (4)$$

Here $\Sigma|A_n^+|^2$ is the power transported in the $+z$ direction, $\Sigma|A_n^-|^2$ is the power transported in the $-z$ direction, a is the radius (as a function of z) of the mode converter, x'_{0n} is the nth zero of $J'_0(x)$ excluding the one at $x=0$, and $\beta_n = \sqrt{k^2 - (X'_{0n}/a)^2}$ where k is the free-space wavenumber.

III. Single-Period $TE_{02}-TE_{01}$ Design

From two-mode considerations (TE_{02} and TE_{01}) an estimate of the radial perturbation, $a_1\{1+(\epsilon_1/a_1)[1-\cos(H(z))]\}$, can be made [6]. The perturbation amplitude, ϵ_1/a_1, satisfies the equation

$$\frac{X'_{02}X'_{01}}{X'^2_{02} - X'^2_{01}} 2\pi(\epsilon_1/a_1)\left[1-(\epsilon_1/a_1)+5/4(\epsilon_1/a_1)^2\right] = \pi/2. \quad (5)$$

The function $H(z) = H_0(z) + H_1(z)$, which accounts for the variation of the beat wavenumber, is given by the

Manuscript received October 22, 1990; revised April 25, 1991. This work was supported by the U.S. Department of Energy under Contract DE-FG02-85ER52122 and by the National Magnetic Fusion Energy Computer Center.

M. J. Buckley was with the Department of Electrical and Computer Engineering of the University of Wisconsin, Madison, WI 53706. He is now with the Westinghouse Electric Corporation, Baltimore, MD 21203.

D. A. Stein was with the Department of Electrical and Computer Engineering of the University of Wisconsin, Madison, WI 53706. He is now with the McDonnell Douglas Corporation, St. Louis, MO.

R. J. Vernon is with the Department of Electrical and Computer Engineering of the University of Wisconsin, Madison, WI 53706.

IEEE Log Number 9101368.

0018-9480/91/0800-1301$01.00 ©1991 IEEE

equations

$$H_0(z) = z\left(\frac{X_{02}'^2 - X_{01}'^2}{2ka_1^2\left(1+2(\epsilon_1/a_1)+3/2(\epsilon_1/a_1)^2\right)}\right)\left[1+\frac{X_{02}'^2 + X_{01}'^2}{4a_1^2k^2(1+\epsilon_1/a_1)^2}\right] \quad (6)$$

and

$$H_1(z) = \frac{2\left[(\epsilon_1/a_1)+(\epsilon_1/a_1)^2\right]\sin(H_0)-1/4(\epsilon_1/a_1)^2\sin(2H_0)}{1+2(\epsilon_1/a_1)+3/2(\epsilon_1/a_1)^2} \quad (7)$$

where, for a single-period device, $0 \leqslant H(z) \leqslant 2\pi$.

Because of the short length of the device and hence the large perturbation amplitude, coupling to higher order modes is quite large. In order to suppress higher order mode coupling, the radial perturbation given above was extensively modified. The radial perturbation modifications were determined by numerically solving the coupled mode equations. Five modes, TE_{01} through TE_{05}, were used in the numerical analysis. The radial variation of a one-period TE_{02}–TE_{01} mode converter having a computed conversion efficiency of 97.6% is

$$\begin{aligned} a(z) = 0.01389\{&1+0.42[1-0.39\cos(20.9z)] \\ &\cdot[1-\cos(34.9z+B_1\sin(34.9z) \\ &+0.2\sin(69.8z))] \\ &-0.043[1+0.6\cos(44.72z)][1-\cos(34.9z)] \\ &+E_2[1-\cos(87.3z)]\}m \end{aligned} \quad (8)$$

where $0 \leqslant z \leqslant 0.144m$,

$$B_1 = \begin{matrix} 0.85 & \text{if } z \leqslant 0.09m \\ 1.07 & \text{if } z > 0.09m \end{matrix}$$

and

$$E_2 = \begin{matrix} 0.014 & \text{if } z \leqslant 0.144m \\ 0 & \text{if } z > 0.144m. \end{matrix}$$

Fig. 1 shows this wall profile and Fig. 2 is a graph of computed modal amplitude as a function of position along this mode converter. Fig. 3 is a plot of conversion efficiency as a function of frequency.

IV. Reflection

The coupled-mode equations incorporating both forward- and backward-traveling waves constitute a two-point boundary value problem. The incoming waves at the beginning of the waveguide are known and the reflected waves at the end of the waveguide are assumed to be zero. In this section, a technique for calculating the power reflected from mode converters will be presented. The technique is based on work done by Bellman and Wing [5]. Their approach results in the conversion of a two-point boundary value problem into an initial value problem.

Fig. 4 shows a perturbed waveguide of length L. The beginning of the waveguide is located at the coordinate point zero and the end of the waveguide is located at the coordinate point L. The modal input to the waveguide is denoted by the column vector $\underline{y}$. The power flowing in the $+z$ direction at the point z is given by $|\underline{A}^+(z,\underline{y})|^2$. The power flowing in the $-z$ direction at the point z is given by $|\underline{A}^-(z,\underline{y})|^2$. In the derivation that follows, the length of the perturbed waveguide will vary, while the input $\underline{y}$ will remain constant.

For a given input $\underline{y}$, we seek to determine the transmitted vector $\underline{t}(L,\underline{y})$ and the reflected vector $\underline{r}(L,\underline{y})$, where $|\underline{t}(L,\underline{y})|^2$ is the power traveling in the $+z$ direction at the end of a perturbed waveguide of length L and $|\underline{r}(L,\underline{y})|^2$ is the power traveling in the $-z$ direction at the beginning of a perturbed waveguide of length L.

In order to derive differential equations for $\underline{r}$ and $\underline{t}$, the section of the perturbed waveguide shown in Fig. 4 will be considered in Fig. 5. The section of perturbed waveguide will be lengthened a small distance Δ and the coupled mode equations will be manipulated to yield differential equations for $\underline{r}$ and $\underline{t}$ (see Fig. 6).

In finite difference form, the coupled mode equations can be written as

$$\underline{A}^+(z,\underline{y}) - \underline{A}^+(z-\Delta,\underline{y}) = \Delta\{[T^+(z)]\underline{A}^+(z,\underline{y}) + [\Gamma^-(z)]\underline{A}^-(z,\underline{y})\}$$

and

$$\underline{A}^-(z,\underline{y}) - \underline{A}^-(z-\Delta,\underline{y}) = \Delta\{[\Gamma^+(z)]\underline{A}^+(z,\underline{y}) + [T^-(z)]\underline{A}^-(z,\underline{y})\}$$

where $[T^+(z)]$ denotes the matrix of the coefficients coupling modes both propagating in the $+z$ direction, $[\Gamma^-(z)]$ denotes the matrix of the coefficients coupling modes propagating in the $-z$ direction with modes propagating in the $+z$ direction, $[\Gamma^+(z)]$ denotes the matrix of coefficients coupling modes propagating in the $+z$ direction with modes propagating in the $-z$ direction, and $[T^-(z)]$ denotes the matrix of coefficients coupling modes both propagating in the $-z$ direction. At the beginning of the section of perturbed waveguide,

$$\underline{A}^-(z_1,\underline{y}) = \underline{r}(L-z_1,\underline{y}')$$

$$\underline{A}^-(z_1-\Delta,\underline{y}) = \underline{r}(L+\Delta-z_1,\underline{y})$$

$$\underline{A}^+(z_1,\underline{y}) = \underline{y}' \quad \text{and} \quad \underline{A}^+(z_1-\Delta,\underline{y}) = \underline{y}.$$

Since the perturbed waveguide is a linear system, $\underline{r}(L+\Delta-z,\underline{y}) = [r(L+\Delta-z)]\underline{y}$, where $[r(L+\Delta-z)]$ is the reflection matrix for a waveguide of length $L+\Delta-z$. In finite difference form the coupled mode equations can be rewritten as

$$\underline{y}' - \underline{y} = \Delta\{[T^+]\underline{y} + [\Gamma^-][r(L-z_1)]\underline{y}\} \quad (9)$$

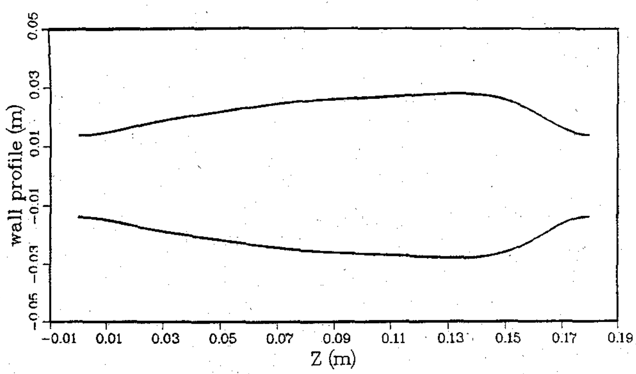

Fig. 1. Wall profile for the 60 GHz single-period TE_{01}–TE_{02} mode converter.

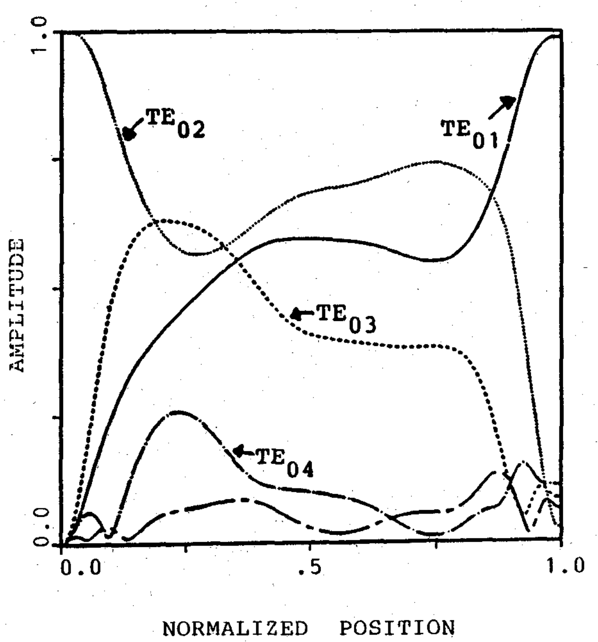

Fig. 2. Normalized modal amplitude as a function of position along the 60 GHz single-period TE_{02}–TE_{01} mode converter. The amplitude is normalized so that its square gives the local fraction of power carried by that particular mode. The computed conversion efficiency of the mode converter is 97.6%

and

$$[r(L-z_1)]\underline{y}'-[r(L-z_1+\Delta)]\underline{y} = \Delta\{[\Gamma^+]\underline{y}'+[T^-][r(L-z_1)]\underline{y}\}. \quad (10)$$

Since only terms of order Δ are being retained, $\underline{y}'$ on the right-hand side of (10) can be replaced with $\underline{y}$, and $\underline{y}'$ on the left-hand side of (10) can be replaced with $\underline{y}+\Delta([T^+]\underline{y}+[\Gamma^-][r(L-z_1)]\underline{y})$.

Simplifying (10) and taking the limit as $\Delta\to 0$ yields

$$\frac{d}{dz}[r(z)]=\{[\Gamma^+]+[T^-][r]-[r][T^+]-[r][\Gamma^-][r]\}. \quad (11)$$

Similarly, noting that $\underline{t}(L-z_1,\underline{y}')=\underline{t}(L-z_1+\Delta,\underline{y})$ and

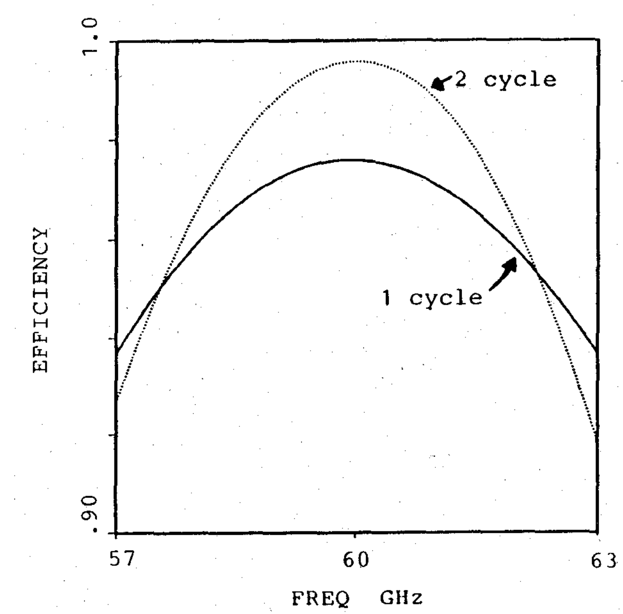

Fig. 3. Graph of conversion efficiency as a function of frequency for the 60 GHz one- and two-period 60 GHz TE_{02}–TE_{01} mode converters.

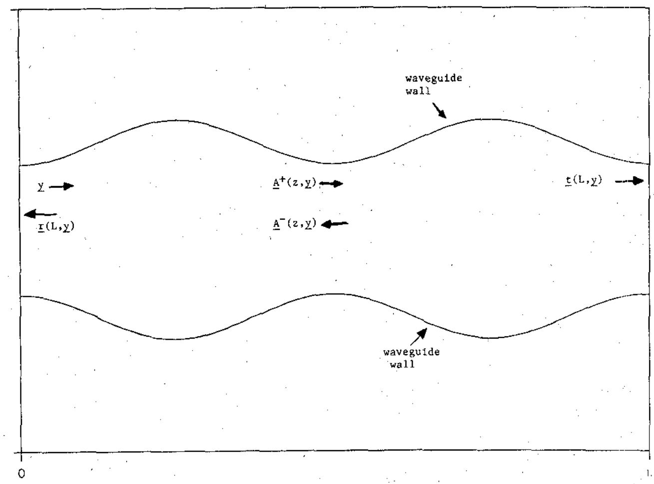

Fig. 4. Schematic diagram of a radial-perturbation mode converter of length L.

proceeding as above leads to

$$\frac{d}{dz}[t(z)]=\{[t][T^+]+[t][\Gamma^-][r]\}. \quad (12)$$

Note that a change of variable has taken place in (11) and (12). The variable of the differentiation is now the coordinate point z. Equations (11) and (12) are initial value problems with initial conditions $[r(L)]=[0]$ and $[t(L)]=[1]$, where [0] is the zero matrix and [1] is the identity matrix.

Equations (11) and (12) can be numerically integrated to determine the reflection amplitude vector $\underline{A}^-(0)$. Table I lists the reflected power for the single-period 60 GHz TE_{02}–TE_{01} mode converter and converters from [6]. In all cases, the reflected power is negligible. Once $\underline{A}^-(0)$ is known, the original coupled mode equations can be treated as an initial value problem and integrated to yield

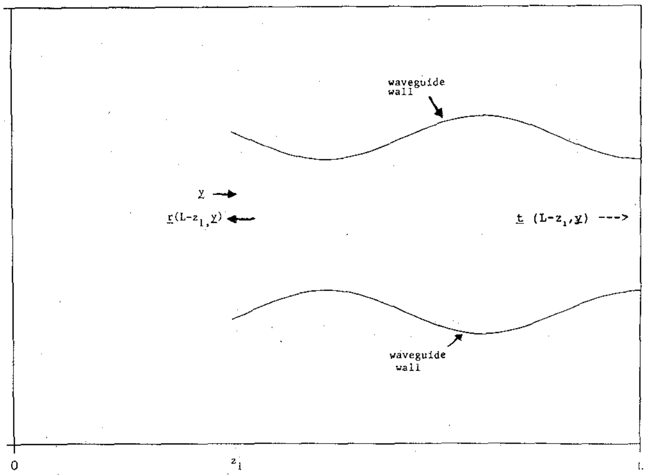

Fig. 5. Schematic diagram of a section of a radial-perturbation mode converter. The length of the section is $L - z_1$.

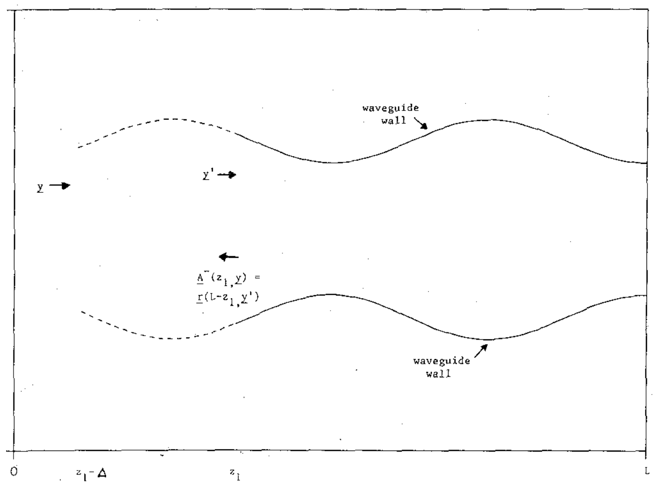

Fig. 6. The waveguide section of Fig. 5 shown lengthened by an amount Δ.

TABLE I
COMPUTED TOTAL REFLECTED POWER FROM SEVERAL TE_{0n} MODE CONVERTER PROFILES

Device	Reflected Power
60 GHz TE_{02}–TE_{01} 2-Period Converter	2.1×10^{-5}%
60 GHz TE_{02}–TE_{01} $1\frac{1}{2}$-Period Converter	7.9×10^{-7}%
150 GHz TE_{02}–TE_{01} 2-Period Converter	3.8×10^{-12}%
60 GHz TE_{02}–TE_{01} $1\frac{1}{2}$-Period Converter	3.8×10^{-12}%
140 GHz TE_{03}–TE_{01} Converter-Taper	3.4×10^{-10}%
60 GHz TE_{02}–TE_{01} Single-Period Converter	8.98×10^{-4}%

a consistency check between (1) and (2) and between (11) and (12).

V. Experimental Results

A single-period mode converter (Fig. 7) with the radius perturbation profile given by (8) was fabricated and tested by two methods: by measuring the far-field radiation pattern [7]–[9] and by using a k-spectrometer [10]. By measuring the far-field radiation pattern of the converter,

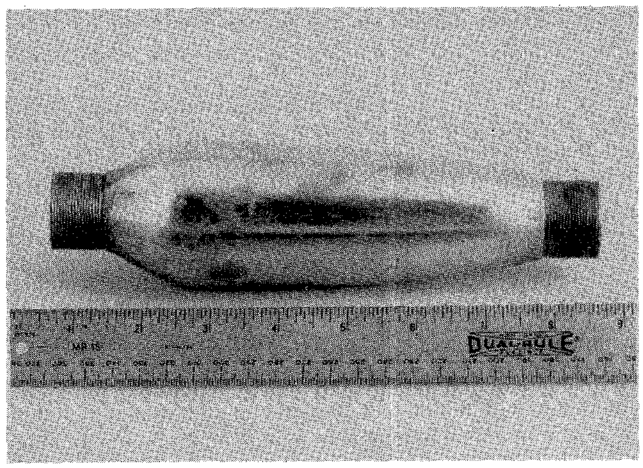

Fig. 7. Photograph of the 60 GHz single-period TE_{02}–TE_{01} mode converter.

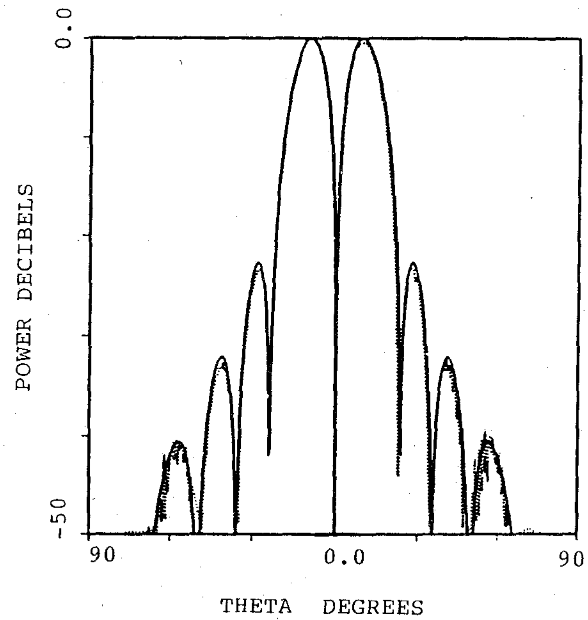

Fig. 8. Graph of the theoretical (solid curve) and measured (dotted curve) radiation pattern of the TE_{01} mode input to the single-period TE_{02}–TE_{01} mode converter.

the power distribution among the transmitted modes can often be determined if they have sufficient amplitude. The k-spectrometer was used to more accurately determine the transmitted mode amplitudes and to obtain an upper limit on the reflected mode amplitudes.

In order to measure the fields radiated from the single-period converter, a TE_{01} mode was applied to the TE_{01} end. From the Lorentz reciprocity theorem [11], the fraction of TE_{02} mode at the TE_{02} end of the converter when a TE_{01} mode is applied to the TE_{01} end is equal to the fraction of TE_{01} mode at the TE_{01} end when a TE_{02} mode is applied to the TE_{02} end. Fig. 8 shows a comparison of the theoretical [9] and experimental far-field radiation patterns of the input TE_{01} mode. Fig. 9 is a comparison of the experimental and theoretical patterns from the single-period converter when a TE_{01} mode is

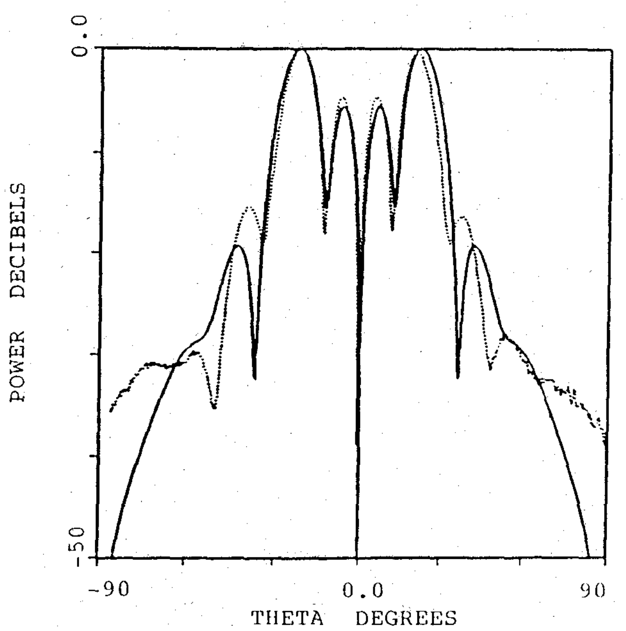

Fig. 9. Graph of the theoretical (solid curve) and measured (dotted curve) radiation pattern of the TE_{02} mode output from the single-period TE_{02}–TE_{01} mode converter.

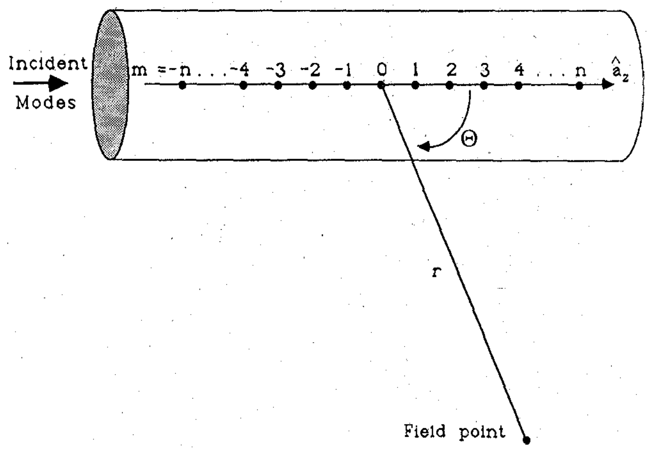

Fig. 10. Schematic drawing of the k-spectrometer.

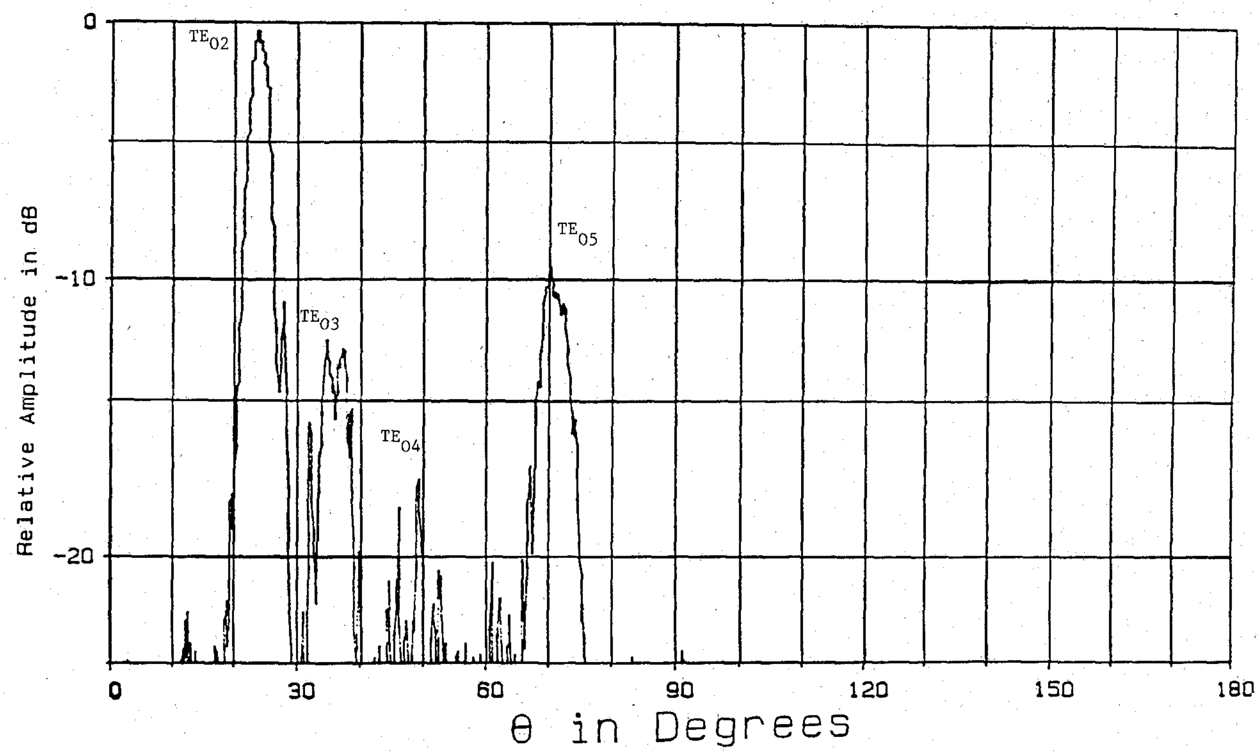

Fig. 11. Radiation pattern from the k-spectrometer with an input from the TE_{02} end of the single-period TE_{02}–TE_{01} mode converter which in turn was excited by a TE_{01} mode at the TE_{01} end.

applied to the TE_{01} end of the converter. The theoretical mode content was calculated by numerically integrating the coupled mode equations. Agreement between theory and experiment is reasonably good over the first two lobes. Some difficulty was encountered in fabricating this converter, which we believe is in part responsible for the disagreement between theory and experiment. It is difficult to accurately determine the spurious mode content from open-end radiation pattern measurements when their power levels are less than about 2% of that of the main mode. This was determined to be the case for the mode converter being discussed.

In order to obtain a somewhat more accurate estimate of the mode converter's conversion efficiency as well as to test for the presence of reflected modes, a preliminary version of a k-spectrometer was designed and fabricated. A k-spectrometer, shown schematically in Fig. 10, is a section of uniform waveguide with a number of apertures

TABLE II
APPROXIMATE PERCENTAGES OF MODES PRESENT AT THE TE_{02} END OF THE SINGLE-PERIOD $TE_{02}-TE_{01}$ MODE CONVERTER FOR A TE_{01} MODE INPUT AT THE TE_{01} END AS DETERMINED FROM K-SPECTROMETER DATA

Mode	Mode Content Determined from k-Spectrometer Data
TE_{01}	1.8%
TE_{02}	96.558%
TE_{03}	1.2%
TE_{04}	0.01%
TE_{05}	0.44%

drilled longitudinally along the guide with uniform spacing. Modes with different phase constants produce radiation patterns with main lobes at different angles, allowing for the determination of the mode content within the waveguide. Modes traveling in the positive z direction produce main lobes in the range $0° < \theta < 90°$ while those traveling in the negative z direction produce main lobes in the range $90° < \theta < 180°$. The radiation pattern from our first version of a k-spectrometer is shown in Fig. 11 for the singled-period mode converter. The higher order TE_{0n} modes carrying the same power excite progressively larger amplitude radiation patterns from a k-spectrometer. Thus the higher order modes appear to have exaggerated amplitudes in Fig. 11. A calibration factor must be applied to obtain the correct approximate amplitude of each mode. Table II shows the approximate amplitude of each mode as estimated from the k-spectrometer radiation pattern.

Finally, the single-period $TE_{02}-TE_{01}$ mode converter was placed after the k-spectrometer to look for the presence of reflected modes. The mode converter was terminated in a matched load. No reflected mode lobes were observed, indicating that any reflected modes were at least 20 dB below the input power level.

VI. CONCLUSIONS

Several important conclusions can be drawn from the computer simulation and measurements on the $TE_{02}-TE_{01}$ mode converter design presented in this paper. First, a single-period varying-radius-type mode converter with reasonably high conversion efficiency is possible under certain conditions even for highly overmoded waveguides. This is a particularly important result since the entire concept of mode selective interference behind the periodic perturbation mode converter is no longer meaningful. This device must be viewed as a mode-selective-profile-type converter since it does not have even qualitative periodicity. Second, varying-radius mode converters with radius increases of more than 50% can be successfully designed. Finally, in highly overmoded waveguides, even these large radius changes do not result in significant reflection.

REFERENCES

[1] C. Moeller, "Mode converters used in Doublet III ECH microwave systems," *Int. J. Electron.*, vol. 53, pp. 587–593, 1982.
[2] H. Kumric and M. Thumm, "Optimized overmoded $TE_{01}-TE_{11}$ mode converters for high-power millimeter wave applications at 70 and 140 GHz," *Int. J. Inf. and Millimeter Waves,* vol. 10, pp. 1439–1463, 1986.
[3] M. Thumm, H. Kumric, and H. Stickel, "$TE_{03}-TE_{01}$ mode converters for use with a 150 GHz gyrotron," *Int. J. Inf. and Millimeter Waves*, vol. 3, pp. 227–240, 1987.
[4] H. G. Unger, "Circular waveguide taper of improved design," *Bell Syst. Tech. J.*, vol. 37, pp. 899–912, 1988.
[5] R. Bellman and G. Wing, *An Introduction to Invariant Imbedding*. New York: Wiley, 1975, pp. 25–28.
[6] M. J. Buckley and R. J. Vernon, "Compact quasi-periodic and aperiodic TE_{0n} mode converters in overmoded circular waveguides for use with gyrotrons," *IEEE Trans. Microwave Theory Tech.*, vol. 38, pp. 712–721, 1990.
[7] Z. X. Zhang *et al.* "Mode analysis of gyrotron radiation by far field measurements," in *Proc. Int. Conf. Infrared and MM Waves*, 1983.
[8] R. J. Vernon, W. R. Pickles, M. J. Buckley, F. Firouzbakht, and J. A. Lorbeck, "Mode content determination of overmoded circular waveguides by open-end radiation pattern measurement," in *Proc. IEEE AP-S Int. Symp.* (Blacksburg, VA), June 1987.
[9] S. Silver, Ed., *Microwave Antenna Theory and Design* (MIT Radiation Laboratory Series, vol. 12). New York: McGraw-Hill, 1949, pp. 336–338.
[10] W. Kasparek and G. A. Muller, "The wavenumber spectrometer—An alternative to the directional coupler for multimode analysis in oversized waveguides," *Int. J. Electron.*, vol. 65, pp. 5–20, 1988.
[11] R. E. Collin, *Foundations for Microwave Engineering*. New York: McGraw-Hill, 1966, pp. 172–174.

Michael J. Buckley (S'88–M'88) received the B.S. degree in physics from the College of William and Mary in 1982 and the M.S. and Ph.D. degrees in electrical engineering from the University of Wisconsin in 1984 and 1988 respectively. At the University of Wisconsin, his research interests included mode coupling and mode conversion in overmoded waveguides and radiation from overmoded waveguides.

From August 1988 through February 1990, he was with the Antenna Department of Texas Instruments in McKinney, TX. In February 1990, he joined the Antenna Department of the Westinghouse Electric Corporation in Baltimore, MD, where his research interests include the analysis and design of radomes.

Dr. Buckley is a member of Phi Beta Kappa.

David A. Stein, photograph and biography not available at the time of publication.

Ronald J. Vernon (S'64–M'65) was born in Chicago, IL, on June 3, 1936. He received the B.S., M.S., and Ph.D. degrees in electrical engineering from Northwestern University, Evanston, IL, in 1959, 1961, and 1965 respectively.

He worked under a cooperative student program in the Remote Control Engineering Division of Argonne National Laboratory from 1955 to 1958. Later he worked during the summer as an electrical engineer in the Communications and Industrial Electronics Division of Motorola Inc. Since 1965, he has been on the faculty of the University of Wisconsin, Madison, where he is presently a Professor of Electrical and Computer Engineering. In 1976 and 1977 he took a leave of absence to work at Lawrence Livermore National Laboratory. His current research interests are the development of transmission and mode conversion systems for high-power microwave tubes such as gyrotrons.

Dr. Vernon is a member of Sigma Xi, Tau Beta Pi, Eta Kappa Nu, and Pi Mu Epsilon.